Journal of Reproduction and Development, Vol. 62, No 2, 2016

—Original Article—

Stage-dependent remodeling of the nuclear envelope and lamina during rabbit early embryonic development

Jens POPKEN[1, 2], Volker J. SCHMID[3], Axel STRAUSS[4], Tuna GUENGOER[2], Eckhard WOLF[2] and Valeri ZAKHARTCHENKO[2]

[1]*Division of Anthropology and Human Genetics, Biocenter, LMU Munich, D-82152 Planegg-Martinsried, Germany*
[2]*Chair for Molecular Animal Breeding and Biotechnology, and Laboratory for Functional Genome Analysis (LAFUGA), Gene Center, LMU Munich, D-81377 Munich, Germany*
[3]*Institute of Statistics, LMU Munich, D-80539 Munich, Germany*
[4]*Division of Genetics, Biocenter, LMU Munich, D-82152 Planegg-Martinsried, Germany*

Abstract. Utilizing 3D structured illumination microscopy, we investigated the quality and quantity of nuclear invaginations and the distribution of nuclear pores during rabbit early embryonic development and identified the exact time point of nucleoporin 153 (NUP153) association with chromatin during mitosis. Contrary to bovine early embryonic nuclei, featuring almost exclusively nuclear invaginations containing a small volume of cytoplasm, nuclei in rabbit early embryonic stages show additionally numerous invaginations containing a large volume of cytoplasm. Small-volume invaginations frequently emanated from large-volume nuclear invaginations but not *vice versa*, indicating a different underlying mechanism. Large- and small-volume nuclear envelope invaginations required the presence of chromatin, as they were restricted to chromatin-positive areas. The chromatin-free contact areas between nucleolar precursor bodies (NPBs) and large-volume invaginations were free of nuclear pores. Small-volume invaginations were not in contact with NPBs. The number of invaginations and isolated intranuclear vesicles per nucleus peaked at the 4-cell stage. At this stage, the nuclear surface showed highly concentrated clusters of nuclear pores surrounded by areas free of nuclear pores. Isolated intranuclear lamina vesicles were usually NUP153 negative. Cytoplasmic, randomly distributed NUP153-positive clusters were highly abundant at the zygote stage and decreased in number until they were almost absent at the 8-cell stage and later. These large NUP153 clusters may represent a maternally provided NUP153 deposit, but they were not visible as clusters during mitosis. Major genome activation at the 8- to 16-cell stage may mark the switch from a necessity for a deposit to on-demand production. NUP153 association with chromatin is initiated during metaphase before the initiation of the regeneration of the lamina. To our knowledge, the present study demonstrates for the first time major remodeling of the nuclear envelope and its underlying lamina during rabbit preimplantation development.

Key words: Nuclear envelope, Nuclear lamina, Rabbit embryos

(**J. Reprod. Dev. 62:** 127–135, 2016)

Preimplantation development of rabbit embryos is accompanied by a reduction of nuclear volumes and activation of the embryonic genome [1]. During oogenesis, maternal mRNAs and proteins are deposited into the developing oocyte. After fertilization, this deposit is used to support the initial stages of embryonic development [2]. Before these deposits are depleted, the embryonic genome is activated to produce embryonic mRNAs and proteins for further development. During early development of rabbit embryos, limited transcriptional activity is initiated at the zygote stage and is progressively increased in subsequent stages [3–5], while most genes get activated during major embryonic genome activation (MGA) at the 8- to 16-cell stage [1].

Received: July 16, 2015
Accepted: November 5, 2015
Published online in J-STAGE: December 4, 2015

Correspondence: V Zakhartchenko (e-mail: V.Zakhartchenko@gen.vet-med.uni-muenchen.de)

Nuclear export of newly synthesized mRNAs packaged into messenger ribonucleoprotein (mRNP) complexes is mostly facilitated through nuclear pore complexes (NPCs) [6]. Eight clusters, each containing about 30 nucleoporins (NUPs) [7], are combined to form one NPC with an outer diameter of about 120 nm. A short tunnel in the center of NPCs connects the cytoplasmic ring at the outer membrane with the nuclear ring at the inner membrane of the bilayer lipid nuclear envelope [8]. A more interior terminal ring connected to the nuclear ring by fibers forms the nuclear basket [9]. The nucleoporin NUP153 is localized either at the nuclear ring or at the nuclear basket [10]. Chromatin can associate with the nuclear basket and its attached intranuclear filaments [9].

The nuclear envelope is separated from chromatin by the nuclear lamina. In developing cells, the lamina is made up of lamins B1 and B2, whereas differentiated cells feature lamins A and C [11]. The lamina is required by NPCs for nuclear envelope insertion [12]. Invaginations of the nuclear envelope and the nuclear lamina can extend the import/export functionality of nuclear pores to regions remote from the nuclear surface [13,14]. During early embryonic development, the volume and surface of initially large nuclei decline.

Previously, we studied the changes of the nuclear envelope, nuclear pores and nuclear lamina in bovine preimplantation embryos [15]. Major findings included the presence of NPC-free areas in chromatin-free areas of the envelope up to MGA, three different types of invaginations (lamin B+/NUP153+, lamin B+/NUP153- and lamin B-/NUP153+) and large, randomly distributed NUP153 clusters in the cytoplasm before the onset of MGA correlating with NUP153 spliced mRNA deposits in oocytes. In this study, we compared these findings with the situation in rabbits, since rabbit nuclei can have a far more invaginated nuclear envelope than the generally round bovine nuclei.

Materials and Methods

Ethics statement

Female rabbits were mated with males and slaughtered for embryo recovery. No animal experiments were conducted.

Embryo culture

In vivo fertilized zygotes were flushed from the oviducts 18–20 h post-hCG injection in warm phosphate buffered saline (PBS) supplemented with 4 mg/ml bovine serum albumin and then cultured in Quinn's medium containing 2.5% fetal calf serum in a humidified atmosphere of 5% CO_2 in air at 38.5ºC until the appropriate stage for fixation.

Fixation of embryos

Unless noted otherwise, fixation of embryos and all subsequent steps were performed at room temperature. Embryos were briefly washed in 38ºC PBS, fixed in 2% paraformaldehyde (PFA) in PBS, washed twice in PBS and then stored at 4ºC in PBS until further use.

Immunostaining and embedding

Background caused by PFA was quenched using 20 mM glycine in PBS for 10 min. After washing twice with PBS, embryos were permeabilized with 0.5% Triton-X 100 for 15–30 min. After washing twice with PBS, unspecific background signals were reduced by incubation in 2% BSA for 2 h. Embryos were sequentially incubated in 40 µl of primary and secondary antibody solutions, diluted as specified in Tables 1 and 2 in PBS with 2% BSA. Specimens were incubated with primary antibodies overnight at 4ºC. After washing 5 × in PBS with 2% BSA, the appropriate secondary antibodies, diluted in PBS with 2% BSA, were applied for 1 h, followed by 5 × washing in PBS with 2% BSA and 5 × washing without BSA. Thereafter fixation of antibodies was performed with 4% PFA in PBS for 10 min, followed by washing twice in PBS. Before removal of the zona pellucida, chromatin was counterstained with DAPI (4′,6-diamidino-2-phenylindole, catalog No. D1306, Life Technologies, Darmstadt, Germany) diluted in PBS (2.5 µg/ml) for 10 min followed by washing twice in PBS. Individual blastomeres were attached to precision cover glasses (18 × 18 mm, 170 ± 5 µm, item no. LH22.1, Carl Roth, Karlsruhe, Germany) in PBS and embedded in Vectashield (Vector Laboratories, Lörrach, Germany).

Three-dimensional confocal laser scanning microscopy (3D-CLSM)

3D-CLSM was performed using a large aperture oil immersion objective (63 × /1.4 NA). If the working distance of this objective was insufficient, an objective with a lower aperture and a longer working distance (20 × /0.7 NA) was used. Light optical serial sections of nuclei were recorded with a Leica TCS SP5 using x,y/z voxel sizes of 30–120 nm/200 nm for imaging of selected nuclei. Fluorochromes were excited with blue diode, argon and helium-neon lasers using laser lines at 405 nm, 488 nm and 594 nm, respectively.

3D structured illumination microscopy (3D-SIM) and quantitative image evaluation

3D-SIM of embryonic nuclei was performed on a DeltaVision OMX V3 system (Applied Precision Imaging/GE Healthcare) with a lateral (x, y) resolution of ~120 nm and an axial (z) resolution of ~300 nm [17]. The system was equipped with a 100 × /1.40 NA PlanApo oil immersion objective (Olympus, Hamburg, Germany), Cascade II:512 EMCCD cameras (Photometrics, Ottobrun, Germany) and 405, 488 and 593 nm diode lasers. Image stacks were acquired with a z-distance of 125 nm and with 15 raw SIM images per plane (5 phases, 3 angles). The SI raw data were computationally reconstructed with channel-specific measured OTFs using the softWoRX 4.0 software package (Applied Precision). Images from the different color channels were registered with alignment parameters obtained from calibration measurements with 0.2 µm diameter TetraSpeck beads (Invitrogen, Darmstadt, Germany). The voxel size of the reconstructed images is 39.5 nm in x and y and 125 nm in z with a 32-bit depth. For all subsequent image processing and data analyses, images were converted to 16-bit composite tiff stacks. Image stacks were processed using ImageJ 1.45b (http://rsb.info.nih.gov/ij/). Images are shown after application of a threshold, which removed background, including patterns apparently resulting from SIM imaging/reconstruction [16]. DAPI intensity classes were established as described previously [17]. Statistical comparisons were performed with the software package for scientific computing R 2.15 (http://www.r-project.org/).

Results

The stage-dependent changes in the distribution of NUP153, NPCs, the nuclear lamina, isolated intranuclear laminar vesicles and nuclear envelope invaginations were studied with 3D-SIM of zygote- to blastocyst-stage embryos stained for chromatin (DAPI) and immunostained for NUP153 and lamin B. We scanned and analyzed 112 pronuclei/nuclei in 28 embryos.

Distribution of chromatin, NUP153 and lamin B changes at the beginning of preimplantation development

Early embryonic development is characterized by profound changes in the distribution of chromatin and nuclear pores (Fig. 1). At the zygote stage, smaller female pronuclei (fPN) with an evenly shaped nuclear border and larger male pronuclei (mPN) with a more wave-like nuclear border were always located in close association with each other. Contrary to mPN, fPN showed a chromatin gradient from a large concentration at the mPN contact area to a small concentration at the area most remote from the contact site. The nuclear envelope

Table 1. Primary antibodies

Host	Target	Official name	Dilution	Company	ID
Goat	Epitope at C-terminus of Lamin B1. Detecting Lamin B1 and, to a lesser extent, Lamin B2	Lamin B Antibody (M-20)	1:100	Santa Cruz	Santa Cruz
Mouse	NUP153	Anti-NUP153 [QE5] antibody	1:200	Santa Cruz	Santa Cruz

Table 2. Secondary antibodies

Host	Target	Fluorophore	Excitation [nm]	Dilution	Company	ID
Donkey	Mouse IgG (H+L)	Alexa	488	1:400	Invitrogen	A-21202
Donkey	Mouse IgG (H+L)	Alexa	594	1:500	Invitrogen	A-21203
Donkey	Goat IgG (H+L)	Alexa	488	1:400	Invitrogen	A-11055
Donkey	Goat IgG (H+L) preadsorbed	Alexa	594	1:400	Abcam	ab150136

at this remote area was free of NPCs, whereas the nuclear border in contact with the mPN was enriched with NPCs. Both areas of the nuclear border were lamin B positive. Invaginations of the nuclear border were restricted to chromatin-positive areas. Both fPN and mPN feature a large amount of short, small-volume invaginations positive for lamin B and NUP153. In addition, fPN feature the long, large-volume invaginations at the mPN contact site most common for all subsequent stages in the rabbit. Early 2-cell stage nuclei showed a chromatin-free lacuna, whereas nuclei at the end of the 2-cell stage and subsequent stages no longer showed a round lacuna. With the onset of MGA at the 8- to 16-cell stage, the chromatin was more clustered in individual patches (Fig. 2) until the chromatin distribution became more evenly distributed throughout the nucleus at the blastocyst stage.

Long, voluminous invaginations can ensure proximity to cytoplasm for nucleolar precursor bodies

Rabbit nuclei displayed two types of invaginations. The most common type of invaginations contained large volumes of cytoplasm (Fig. 3A–D). These invaginations could reach across nuclei, connect opposing nuclear borders and subdivide into more voluminous invaginations. The other type of invaginations contained barely any volume (arrowheads in Fig. 3B). In the zygote stage, large-volume invaginations were limited to the area where the two pronuclei were in contact, whereas small-volume invaginations were limited to all chromatin-positive areas of the pronuclei (Fig. 1A). Small-volume invaginations emanated from the nuclear periphery or from large-volume invaginations.

Most nucleolar precursor bodies (NPBs) were located either close to the nuclear border or close to large-volume invaginations (Fig. 3). NPBs located at the nuclear border could be located in close proximity to large invaginations as well. Rarely, NPBs were located in the nuclear interior without any invaginations in their proximity. Multiple large invaginations could be in proximity to a single NPB. Some NPBs were in direct contact with large-volume invaginations. The contact sites between voluminous invaginations and NPBs usually did not contain NPCs, but NPCs could be located at the contacting invagination in close proximity to contact sites. NPBs were not necessarily in contact with an invagination emanating from the closest nuclear border. In some cases, the entire nucleus was crossed by an invagination emanating from the nuclear border most remote from the NPB it was in contact with.

Three types of intranuclear vesicles

Fig. 3E–G presents the three different types of intranuclear vesicles observed. Intranuclear vesicles are defined as voluminous structures inside the nucleus without a connection between their interior and the cytoplasm. The most common vesicles were positive for lamin B but not for NUP153 (Fig. 3E). Far less common were vesicles positive for both lamin B and NUP153 (Fig. 3F). In only a single case, a NUP153-positive but lamin B-negative vesicle-like structure was observed (Fig. 3G; arrow 2). Usually NUP153-positive structures were lined by chromatin (compare with Fig. 1A). This vesicle was not lined by chromatin. The NUP153 signal strength was much lower than the signal strength of NPCs in the nuclear envelope.

Quantification of nuclear volumes

Generally, nuclear volumes declined with later stages from the 2-cell to the blastocyst stage (Fig. 4A). As exceptions, the 2-cell and morula stages featured a wide variety of nuclear volumes. In a morula-stage embryo, the largest nuclei could be larger than the nuclei of an embryo at the 8-cell stage. These nuclei could not simply be stopped/retarded 8-cell stage nuclei, since more than 8 large nuclei were observed in addition to numerous smaller nuclei in the same morula-stage embryo. Small morula nuclei could have the same size as those of blastocysts.

Invaginations peak at the 4-cell stage

The diagram in Fig. 4B reflects the quantification of invaginations and intranuclear vesicles throughout all developmental stages. The most common invaginations and intranuclear vesicles were positive for both lamin B and NUP153. They were present in all stages. Their

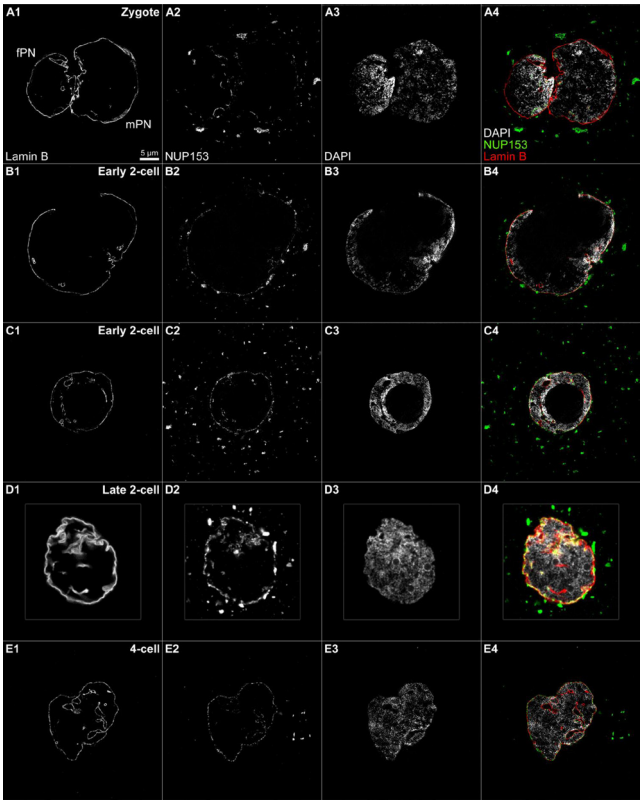

Fig. 1. Nuclear volumes and distribution changes of chromatin, NUP153 and lamin B before MGA. Panels A–E. Midsections of pronuclei/nuclei from rabbit IVF embryos immunostained for lamin B (A1–E1; A4–E4, red) and NUP153 (A2–E2; A4–E4, green) and stained for chromatin with DAPI (A3–E3; A4–E4, gray). A: Zygote stage with a small female pronucleus (fPN) and a large male pronucleus (mPN). B: Early 2-cell stage with a large chromatin-free lacuna. The lacuna is connected to the cytoplasm without a lamin B- or NUP153-positive border. C: Early 2-cell stage with a smaller chromatin-free lacuna surrounded by chromatin. D: Late 2-cell stage without a chromatin-free lacuna recorded with confocal laser scanning microscopy. E: 4-cell stage.

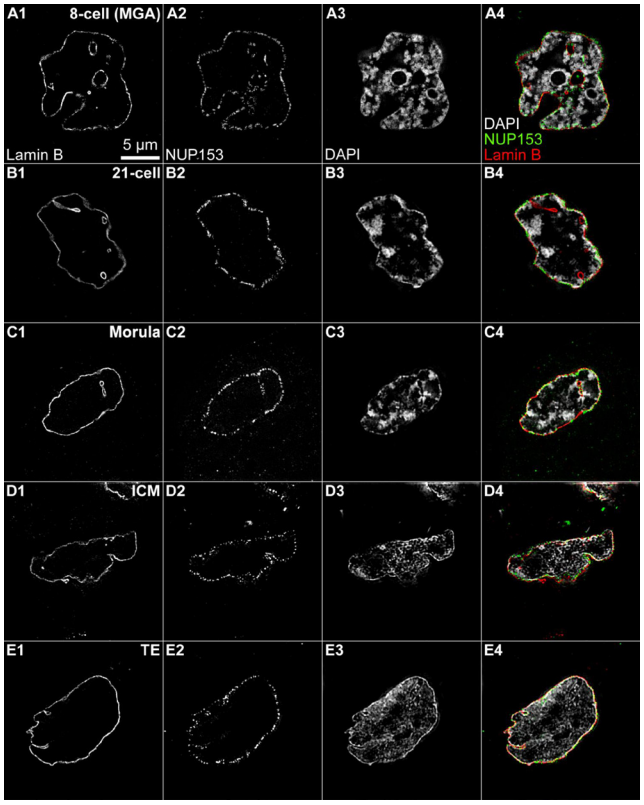

Fig. 2. Nuclear volumes and distribution changes of chromatin, NUP153 and lamin B at the onset of and after MGA. Panels A–E. Midsections of nuclei from rabbit IVF embryos immunostained for lamin B (A1–F1; A4–F4, red) and NUP153 (A2–F2; A4–F4, green) and stained for chromatin with DAPI (A3–F3; A4–F4, gray). A: 8-cell stage. B: 21-cell stage. C: 44-cell morula stage. D: Inner cell mass (ICM) nucleus in a blastocyst-stage embryo. E: Trophectoderm (TE) nucleus in a blastocyst-stage embryo.

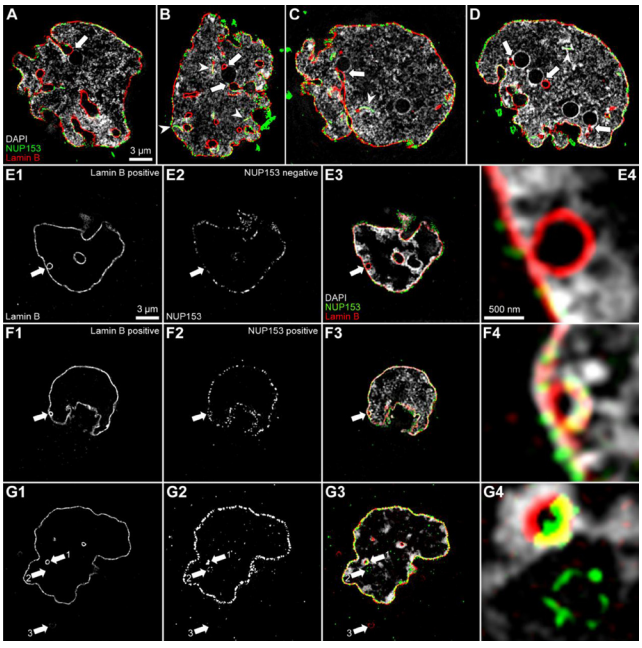

Fig. 3. A–D. Large-volume and small-volume invaginations. A: 4-cell-stage nucleus with a large-volume invagination in contact with a nucleolar precursor body (NPB; the arrow marks the contact site). Note the absence of nuclear pores at the contact site. B: 4-cell-stage nucleus with small-volume invaginations (arrowheads) and multiple large-volume invaginations contacting the same centrally located NPB (arrows mark contact sites between invaginations and the nucleolus). C: 4-cell-stage nucleus with a large-volume invagination reaching across the nucleus to contact a NPB (arrow marks contact site). The arrowhead marks a small-volume invagination emanating from a large-volume invagination. The NPB on the right side is not contacted by any invagination. D: 4-cell-stage nucleus showing three of the four NPBs in contact with large-volume invaginations (contact sites marked by arrows). The NPB not in contact with invaginations is in contact with the nuclear border in another z-section (not shown). E–G: Three types of intranuclear vesicles. E1–G1: Lamin B (3 µm bar). E2–G2: NUP153. E3–G3 and E4–G4: DAPI (gray), NUP153 (green) and Lamin B (red). E4–G4: Magnification of the vesicles (500 nm bar). E: Lamin B-positive but NUP153-negative intranuclear vesicles are most common. F: Lamin B- and NUP153-positive invaginations are far less common. G: Arrow 2 marks the only occurrence of a NUP153-positive but lamin B-negative vesicle-like structure. This may not be a NPC-positive vesicle-like structure, since NPCs are normally lined with chromatin but this structure is not.

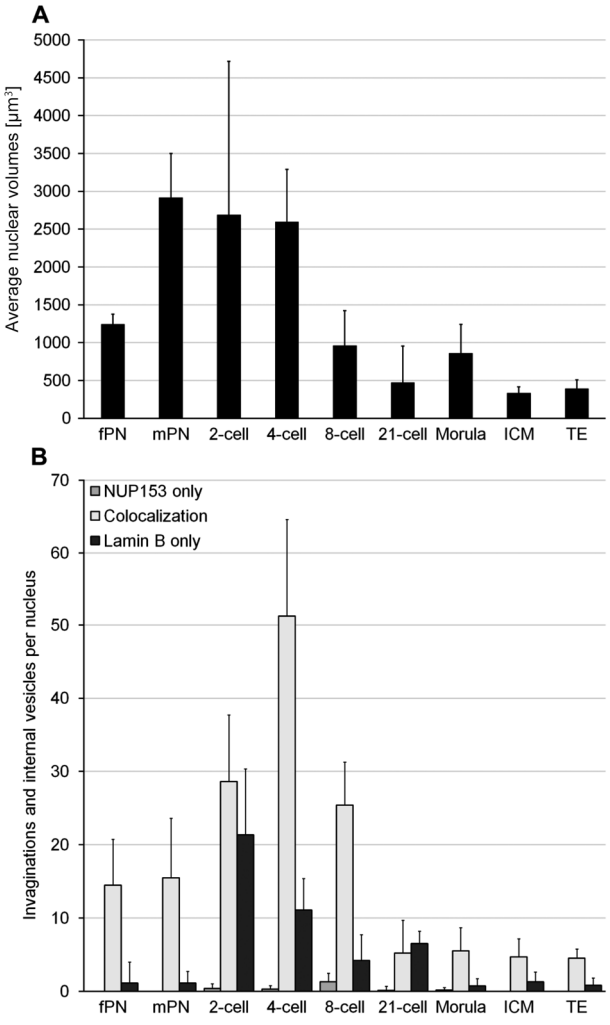

Fig. 4. A: Quantification of nuclear volumes. fPN, female pronucleus; mPN, male pronucleus; ICM, blastocyst nucleus from the inner cell mass; TE, blastocyst nucleus from the trophectoderm. For each bar, 10 pronuclei/nuclei were measured. B: Quantification of invaginations and intranuclear vesicles. For abbreviations, see (A). Exclusively NUP153-positive structures are marked in dark gray. NUP153- and lamin B-positive structures are marked in light gray. Exclusively lamin B-positive structures are marked in black. For each set of bars, invaginations and vesicles in 10 pronuclei/nuclei were counted.

frequency per nucleus increased at each stage from the zygote to the 4-cell stage. After the 4-cell stage, they became less frequent and stagnated at the 21-cell stage to blastocyst stage. The second most frequent invaginations and intranuclear vesicles were lamin B positive but NUP153 negative, which peaked in 2-cell stage nuclei. Stagnation at small levels was reached in morula nuclei. NUP153- positive but lamin B-negative structures were rarely observed.

Maternal deposit of extranuclear NUP153-positive clusters up to MGA

Fig. 5A shows a large deposit of NUP153-positive clusters in the zygote stage. These clusters were reduced in size and abundance during the subsequent stages (Fig. 5B–H). At the 4-cell stage, these clusters were usually limited to areas of the cytoplasm located on one side of the nucleus (Fig. 5C1). This deposit was largely depleted at MGA at the 8- to 16-cell stage and subsequent stages (Fig. 5D–H).

Random distribution of NPCs is initiated at MGA

Figure 6 presents nuclei from a pre-MGA 4-cell stage embryo (Fig. 6A–E) and post-MGA 21-cell stage embryo (Fig. 6F–H). Extranuclear NUP153 clusters in 4-cell stage blastomeres were only localized in the cytoplasm on one side of the nucleus (see Fig. 5C1 for a full projection including extranuclear clusters). This phenomenon allowed for a half-projection, which included only sections from the half of the nucleus in which almost no external NUP153 clusters were present. This half-projection shows NPCs integrated into the nuclear envelope unobstructed by cytoplasmic NUP153 clusters.

In the pre-MGA nucleus, NPCs were mostly clustered in highly concentrated areas. Some areas in these clusters surpassed the resolution limit of 3D-SIM, and multiple NPCs appeared as combined signal clouds. However, adequately resolved isolated nuclear pores in the vicinity of highly concentrated clusters demonstrated that this signal combination was not an artifact of an insufficient image quality. The left arrow in Fig. 6D5 marks isolated nuclear pores, and the right arrow marks a group of tightly clustered NPCs. NPC clusters co-localized with areas of low lamin B signal intensity, indicating reduced abundance of lamin B at the NPC integration site (compare Fig. 6B1/2 and D1/2 with B5/6 and D5/6, respectively). However, NUP153 signals were not always found throughout areas of reduced lamin B signals (arrows in Fig. 6B3/4). This might indicate that other parts of NPCs may still or already be present at an NPC integration site while NUP153 is still or already absent. Similar but isolated NUP153-free small lamin B spots were found in post-MGA nuclei (arrow in Fig. 6H4). Pre-MGA NPC clusters were not evenly distributed and were sometimes separated by larger NPC-free areas. NPCs were only present in areas of the nuclear border that featured at least a thin heterochromatin lining under the lamina. While lamin B signals were also present in areas of the nuclear border without an underlying heterochromatin lining, NPCs were absent in the areas (see arrows in Fig. 6E). NPCs were far less concentrated and no longer isolated as clusters in post-MGA nuclei, while isolated NPCs were more common. However, heterochromatin lining of the nuclear border did not necessarily guarantee NUP153 presence (see arrows in Fig. 6G2).

NUP153 association with chromatids begins at the chromatid periphery during metaphase before reassembly of the nuclear lamina

Fig. 7 displays morula-stage blastomeres during metaphase (A, B) and during anaphase/telophase (C). At one time point during metaphase, both NUP153 and lamin B were enriched in the cytoplasm and underrepresented in chromatids (A8). While the NUP153 distribution in the cytoplasm seems random, multiple lamin B- positive clusters were observed (A3). At another time point during metaphase (B), the distribution of lamin B remained unchanged, while NUP153 was enriched at the periphery of chromatids but underrepresented in the cytoplasm and inside the chromatid interior (B8). During anaphase/telophase (C), the distribution of lamin B

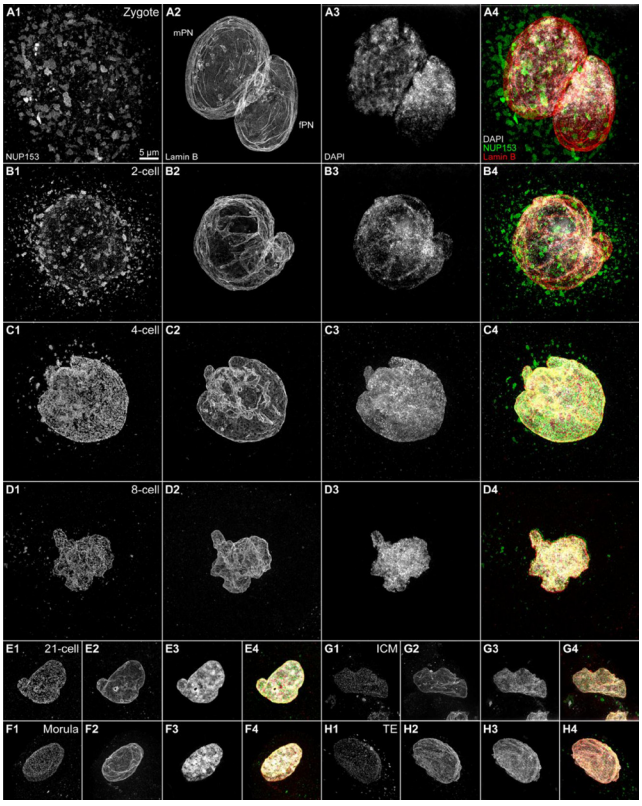

Fig. 5. A maternal deposit of cytoplasmic NUP153 clusters is depleted at the onset of MGA. A1–H1: NUP153. A2–H2: Lamin B. A3–H3: DAPI. A4–H4: Composite (DAPI, gray; NUP153, green; lamin B, red). A: Zygote stage with a large male (mPN) and small female pronucleus (fPN). B: 2-cell stage. C: 4-cell stage. D: 8-cell stage. E: 21-cell stage. F: Morula stage. G: Inner cell mass nucleus from a blastocyst. H: Trophectoderm nucleus from a blastocyst.

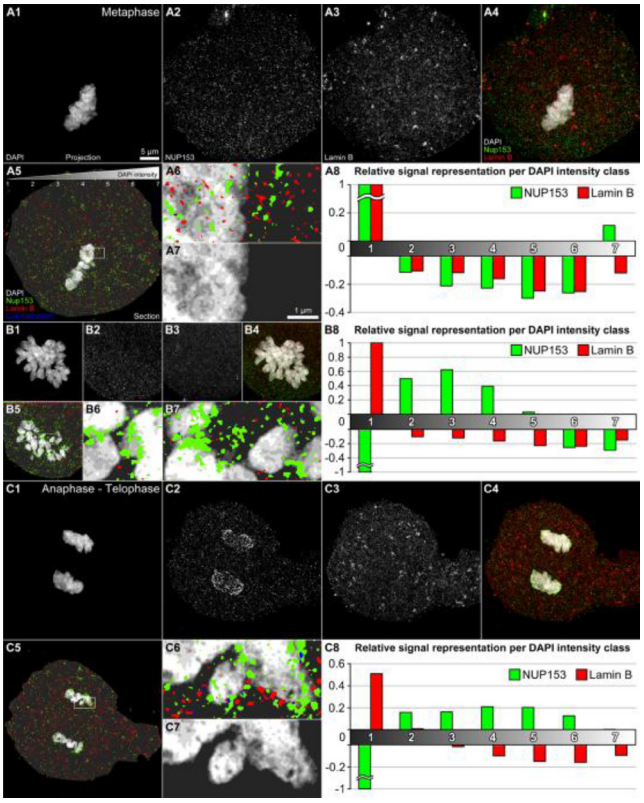

Fig. 7. See figure legend in p. 133.

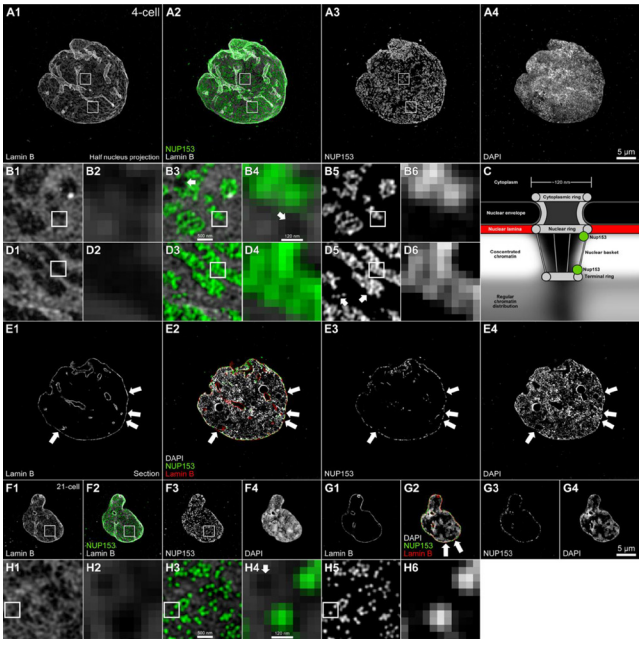

Fig. 6. Nuclear pore complex (NPC) and lamina distribution before and after major genome activation (MGA). A: Projection through half of a pre-MGA 4-cell stage nucleus. A1: Lamin B. A2: Composite with lamin B (gray) and NUP153 (green). A3: NUP153. A4: DAPI. B1: Enlargement of top box in A1. B2: Enlargement of box in B1. B3: Enlargement of top box in A2. The arrow marks a lamin B-depleted area without NPCs. B4: Enlargement of box in B3. The arrow marks a lamin B-depleted area without NPCs. This depleted area is approximately the size of one NPC (120 nm in diameter). B5: Enlargement of top box in A3. B6: Enlargement of box in B5. C: Model of a NPC with potential NUP153 localizations based on the report of Ball and Ullman [10]. NPCs have an outer diameter of about 120 nm and connect the cytoplasm with the nucleoplasm through the nuclear envelope and lamina. The nuclear basket and nuclear filaments connected to the nuclear basket are associated with chromatin. NUP153 is located either at the nuclear ring or at the nuclear basket [10]. D1: Enlargement of bottom box in A1. D2: Enlargement of box in D1. D3: Enlargement of bottom box in A2. D4: Enlargement of box in D3. D5: Enlargement of bottom box in A3. D6: Enlargement of box in B5. E1–E4: Midsection of the nucleus shown in A. Arrows mark areas of the nuclear envelope that feature a lamina but that are lacking chromatin and nuclear pores (compare with the fPN in Fig. 1A). F: Projection through half of a post-MGA 21-cell stage nucleus. G: Midsection of the nucleus shown in F. Arrows mark areas of the nuclear envelope that feature a lamina lined by chromatin but that are lacking nuclear pores. H1, H3, H5: Enlargements of the box in E. H2, H4, H6: Enlargements of the boxes in H1, H3, H5. The arrow in H4 marks a lamin B-depleted area without an NPC. This depleted area is approximately the size of one NPC (120 nm in diameter).

remained unchanged, while NUP153 was underrepresented in the cytoplasm but enriched at the periphery of chromatids and inside the chromatid interior at this stage (C8).

Discussion

This study was initiated to compare the results from our previous investigation on the nuclear envelope, nuclear pores and nuclear lamina in bovine preimplantation embryos [15] with the situation in rabbit embryos, which feature an alternative nuclear phenotype.

Large-volume invaginations provide proximity to cytoplasm for NPBs

While nuclei of bovine early-stage embryos have a round shape with mostly short, small-volume invaginations, early rabbit nuclei feature an amoeba-like shape with mostly large-volume invaginations able to stretch across entire nuclei. A previous study utilizing electron microscopy on *in vivo* and *in vitro* rabbit preimplantation embryos showed similar large-volume invaginations reaching far inside the nucleus [18]. This suggests that these invaginations are not an artifact of the preparation of rabbit embryos for super-resolution fluorescence microscopy. We wanted to compare the composition of nuclear invaginations and the distribution of nuclear pores throughout early embryonic development with the situation we have previously described in the bovine species. Since rabbit embryonic mRNA production peaks at the transition from the morula to blastocyst stage [19, 20], we wanted to investigate whether the increased mRNA production would cause a higher amount of nuclear invaginations despite having smaller nuclear volumes at these later stages. Our results show that nuclear invaginations did not peak at these stages of highest mRNA production. Instead, invaginations positive for NUP153 and lamin B peaked at the 4-cell stage. This stage is the last stage before a massive volume decline begins at the 8-cell stage. This may suggest that a large nuclear volume is a more important factor for a high abundance of invaginations than increased mRNA export.

However, the number of invaginations positive for NUP153 and lamin B was lower at the 2-cell stage and in male pronuclei at the zygote stage, although these pronuclei/nuclei had larger volumes than those at the 4-cell stage. This may indicate that a larger nuclear volume is not the only factor for an increased abundance of invaginations. Nucleologenesis takes place during the first 4 cell cycles, with the first nucleolus-associated RNA of fully functional nucleoli detected at the morula stage containing about 32 cells [21]. Our data show numerous large-volume invaginations competent for import/export in direct contact with NPBs at the 4-cell stage. This may indicate that large-volume invaginations competent for import/export facilitate cytoplasmic proximity to NPBs. A similar association between invaginations and nucleoli in the form of "nucleolar canals" has been shown previously [22, 23]. Fitting this hypothesis, the zygote, 2-cell, 4-cell, and 8-cell stages show the highest amount of nuclear invaginations competent for import/export throughout preimplantation development. The peak of invaginations positive for NUP153 and lamin B at the 4-cell stage may be the result of a combination of large nuclear volumes and a large protein import requirement of NPBs at that particular stage. While nucleologenesis may have been in full progress at the 21-cell stage, the nuclear volumes had already dropped to blastocyst-like levels, and therefore nucleolar proximity to the cytoplasm may have already been sufficient without additional invaginations.

Invaginations exclusively positive for lamin B were associated with nuclear volume reduction

In our previous study on invaginations in bovine nuclei, we hypothesized that import/export-incompetent invaginations only positive for lamin B may be associated with a volume reduction during interphase [15]. A similar process was previously demonstrated during mosquito spermatogenesis, in which vesicle-like excisions of the lamina into the nuclear interior were associated with a reduction of the nuclear surface during interphase [24]. Our hypothesis was based on the fact that this type of invagination was mostly abundant during the 4-, 8- and 19-cell stages, which exhibited strong volume reductions. However, the results of this study show the highest amount of lamin B-only invaginations at the 2-cell stage and a reduction in the numbers of these invaginations in subsequent stages. The results may not be directly comparable between the two studies, since most invaginations in rabbits are large in volume while almost all invaginations in cattle are small-volume invaginations. Nuclear volumes in 2-cell stage nuclei were more variable than in any other preimplantation stage. Due to the lack of live microscopy data, it is not clear whether the same nuclei can vary drastically in volume over time or if small and large nuclei maintain initial volumes throughout the 2-cell stage. However, nuclei at the early 2-cell stage were on average larger and almost always exhibited one or multiple small or large chromatin-free lacunas, whereas nuclei at the late 2-cell stage were on average smaller and no longer exhibited chromatin-free lacunas. This may indicate that during the rabbit 2-cell stage, interphase nuclear volumes are reduced and the chromatin-free lacuna is removed. In this case, the hypothesis of an increased abundance of invaginations exclusively positive for lamin B during interphase nuclear volume reduction would be further substantiated by the results of this study.

Fig. 7. NUP153 associates with chromatids during metaphase before lamina reassembly. A: Lamin B and NUP153 are not associated with chromatids at this time point during metaphase. A1: Projection of DAPI. A2: Projection of NUP153. A3: Projection of lamin B. A4: Projection of a composite of DAPI (gray), NUP153 (green) and lamin B (red). A5: Section showing 7 DAPI intensity classes from no DAPI intensity in the cytoplasm (dark gray) to large DAPI intensity (white), NUP153 (green), lamin B (red) and the colocalization of NUP153 and lamin B (blue). A6: Enlargement of the box in A5. A7: Same enlargement presented in A6 without NUP153, lamin B or colocalization signals. A8: Quantification of over- and underrepresentation of NUP153 (green) and lamin B signals (red) in the 7 DAPI intensity classes. At this stage, NUP153 and lamin B are both strongly overrepresented in the cytoplasm and mostly underrepresented in the chromatin. B1–B8: The descriptions for A1–A8 above also apply to B1–B8, which represent another time point during metaphase. Lamin B remains unassociated with chromatids, but NUP153 begins to associate with the periphery but not the core parts of chromatids during metaphase. C1–C8: The descriptions for A1–A8 above also apply to C1–C8, which represent a time point during anaphase/telophase. Lamin B remains unassociated with chromatids, but NUP153 association stretches into the interior of chromatids during anaphase/telophase.

Different mechanisms for small- and large-volume invaginations

Short, small-volume invaginations, which are the almost exclusive nuclear invagination type in the bovine species, did generally not show association with NPBs. This suggests that there may be a different reason and mechanism responsible for large- and small-volume invaginations in the rabbit species. In the bovine species, small-volume invaginations did emanate from the nuclear border and did not emanate from the few large-volume invaginations. In the rabbit species, numerous small-volume invaginations were emanating from large-volume invaginations. This may imply that import/export-competent large-volume invaginations are essentially similar to the nuclear border. The fact that most NPBs were either located at the nuclear border or at large-volume invaginations further supports this hypothesis. The hypothesis of different roles and mechanisms between small- and large-volume invaginations is further substantiated by the finding that small-volume invaginations were frequently emanating from large-volume invaginations but that large-volume invaginations never emanated from small-volume invaginations.

NUP153 clusters

In our previous study on bovine embryos, we showed large, randomly distributed NUP153 clusters before MGA [15]. After MGA at the 8- to 16-cell stage, these clusters greatly decreased in number and were no longer randomly distributed but were mostly located in close proximity to the nuclear envelope until they were no longer present in morula-stage nuclei. RNA-Seq data showed a deposit of spliced, maternally provided mRNA coding for NUP153, other nucleoporins and lamins already present in oocytes with consistent levels up to the blastocyst stage. In this study, we confirmed the existence of a large deposit of NUP153 clusters randomly distributed throughout the cytoplasm in the rabbit species. Similar to the bovine species, these NUP153 clusters greatly decreased in number at the onset of MGA and were no longer present for the most part at later stages.

NPCs in pre-MGA nuclear envelopes are distributed non-randomly

In a previous study we showed that in nuclei of bovine embryos a large chromatin-free lacuna starts to form at the 4-cell stage and begins to get smaller after MGA at the 8-cell stage [16]. Expansions of this chromatin-free lacuna could be in direct contact with the nuclear border, where we noted a complete lack of nuclear pores. However, chromatin-free areas at the nuclear envelope were already observed at the zygote stage. A similar scenario was noted in this study in rabbit zygotes. A nonhomogeneous chromatin distribution in female pronuclei left half of the nuclear envelope not facing the male pronucleus without visible chromatin. While the entire nuclear envelope was lined by lamin B, this opposing half did not contain NPCs. These chromatin- and NPC-free areas of the nuclear envelope persisted until the 4-cell stage, at which point highly concentrated NPC groups were surrounded by chromatin-free areas exclusively marked by the lamina. This finding confirms the hypothesis that nuclear pores require chromatin.

NUP153 association with chromatids is initiated during metaphase before lamin B association

Previously, the post-mitotic association of NUP153 with chromatin was reported to be initiated at the end of anaphase [25]. In our previous study, this initial association was already observed at metaphase [15]. The difference between these two findings might be explained by increased clustering of NUP153 at the chromatid periphery during anaphase. While a visual inspection using confocal microscopy may suggest that the initial association occurs during anaphase, our statistical analysis of super-resolution data showed that an overrepresentation of NUP153 at the chromatid periphery occurs already during metaphase. Alternatively, there might be species-specific differences. In this study, we were able to show not only that the association between NUP153 and chromatids is already present during metaphase but also that it is initiated during metaphase. Our data confirm for the rabbit species the previous finding that NUP153 association precedes lamina reassembly [25].

Conclusion

Compared with bovine preimplantation development, we found striking differences and similarities. The most profound difference is that most invaginations in rabbits are large-volume invaginations, whereas most invaginations in cattle are small-volume invaginations. Since small-volume invaginations did regularly emanate from large-volume invaginations but large-volume invaginations did not emanate from small-volume invaginations, the underlying mechanism may differ. This is further substantiated by the observation that only large-volume invaginations directly contacted NPBs. Similarities included the lack of NPCs in chromatin-free areas of the nuclear envelope, an increased abundance of invaginations exclusively positive for lamin B during stages with large nuclear volume alterations, deposition of cytoplasmic NUP153 clusters until the onset of MGA and initiation of association of NUP153 with chromatids during metaphase. To our knowledge, the present study demonstrates for the first time major remodeling of the nuclear envelope and its underlying lamina during rabbit preimplantation development.

Acknowledgments

The microscopy work was performed at the Center for Advanced Light Microscopy (CALM) of the LMU Munich.

We gratefully acknowledge the support provided by Thomas Cremer and his critical reading of preliminary versions of the manuscript. This study was supported by grants from the Deutsche Forschungsgemeinschaft to EW and VZ (CR 59/26, FOR 1041, ZA 425/1-3). In addition, research of EW and VZ was supported by the EU grant Plurisys, HEALTH-F4-2009-223485 FP7 Health 534 project. The authors are members of COST Action BM1308 - Sharing Advances on Large Animal Models (SALAAM).

References

1. **Léandri RD, Archilla C, Bui LC, Peynot N, Liu Z, Cabau C, Chastellier A, Renard JP, Duranthon V.** Revealing the dynamics of gene expression during embryonic genome activation and first differentiation in the rabbit embryo with a dedicated array screening. *Physiol Genomics* 2009; **36**: 98–113. [Medline] [CrossRef]
2. **Henrion G, Brunet A, Renard JP, Duranthon V.** Identification of maternal transcripts

that progressively disappear during the cleavage period of rabbit embryos. *Mol Reprod Dev* 1997; **47**: 353–362. [Medline] [CrossRef]

3. **Christians E, Rao VH, Renard JP.** Sequential acquisition of transcriptional control during early embryonic development in the rabbit. *Dev Biol* 1994; **164**: 160–172. [Medline] [CrossRef]
4. **Brunet-Simon A, Henrion G, Renard JP, Duranthon V.** Onset of zygotic transcription and maternal transcript legacy in the rabbit embryo. *Mol Reprod Dev* 2001; **58**: 127–136. [Medline] [CrossRef]
5. **Cotton RW, Manes C, Hamkalo BA.** Electron microscopic analysis of RNA transcription in preimplantation rabbit embryos. *Chromosoma* 1980; **79**: 169–178. [Medline] [CrossRef]
6. **Carmody SR, Wente SR.** mRNA nuclear export at a glance. *J Cell Sci* 2009; **122**: 1933–1937. [Medline] [CrossRef]
7. **Cronshaw JM, Krutchinsky AN, Zhang W, Chait BT, Matunis MJ.** Proteomic analysis of the mammalian nuclear pore complex. *J Cell Biol* 2002; **158**: 915–927. [Medline] [CrossRef]
8. **Hinshaw JE, Carragher BO, Milligan RA.** Architecture and design of the nuclear pore complex. *Cell* 1992; **69**: 1133–1141. [Medline] [CrossRef]
9. **Arlucea J, Andrade R, Alonso R, Aréchaga J.** The nuclear basket of the nuclear pore complex is part of a higher-order filamentous network that is related to chromatin. *J Struct Biol* 1998; **124**: 51–58. [Medline] [CrossRef]
10. **Ball JR, Ullman KS.** Versatility at the nuclear pore complex: lessons learned from the nucleoporin Nup153. *Chromosoma* 2005; **114**: 319–330. [Medline] [CrossRef]
11. **Gruenbaum Y, Margalit A, Goldman RD, Shumaker DK, Wilson KL.** The nuclear lamina comes of age. *Nat Rev Mol Cell Biol* 2005; **6**: 21–31. [Medline] [CrossRef]
12. **Smythe C, Jenkins HE, Hutchison CJ.** Incorporation of the nuclear pore basket protein nup153 into nuclear pore structures is dependent upon lamina assembly: evidence from cell-free extracts of Xenopus eggs. *EMBO J* 2000; **19**: 3918–3931. [Medline] [CrossRef]
13. **Legartová S, Stixová L, Laur O, Kozubek S, Sehnalová P, Bártová E.** Nuclear structures surrounding internal lamin invaginations. *J Cell Biochem* 2014; **115**: 476–487. [Medline] [CrossRef]
14. **Malhas A, Goulbourne C, Vaux DJ.** The nucleoplasmic reticulum: form and function. *Trends Cell Biol* 2011; **21**: 362–373. [Medline] [CrossRef]
15. **Popken J, Graf A, Krebs S, Blum H, Schmid VJ, Strauss A, Guengoer T, Zakhartchenko V, Wolf E, Cremer T.** Remodeling of the nuclear envelope and lamina during bovine preimplantation development and its functional implications. *PLoS ONE* 2015; **10**: e0124619.; DOI 10.1371/journal.pone.0124619. [Medline]
16. **Popken J, Brero A, Koehler D, Schmid VJ, Strauss A, Wuensch A, Guengoer T, Graf A, Krebs S, Blum H, Zakhartchenko V, Wolf E, Cremer T.** Reprogramming of fibroblast nuclei in cloned bovine embryos involves major structural remodeling with both striking similarities and differences to nuclear phenotypes of in vitro fertilized embryos. *Nucleus* 2014; **5-6**: 555–589. [Medline]
17. **Markaki Y, Smeets D, Fiedler S, Schmid VJ, Schermelleh L, Cremer T, Cremer M.** The potential of 3D-FISH and super-resolution structured illumination microscopy for studies of 3D nuclear architecture: 3D structured illumination microscopy of defined chromosomal structures visualized by 3D (immuno)-FISH opens new perspectives for studies of nuclear architecture. *BioEssays* 2012; **34**: 412–426. [Medline] [CrossRef]
18. **Van Blerkom J, Manes C, Daniel JC Jr.** Development of preimplantation rabbit embryos in vivo and in vitro. I. An ultrastructural comparison. *Dev Biol* 1973; **35**: 262–282. [Medline] [CrossRef]
19. **Manes C.** Nucleic acid synthesis in preimplantation rabbit embryos. I. Quantitative aspects, relationship to early morphogenesis and protein synthesis. *J Exp Zool* 1969; **172**: 303–310. [Medline] [CrossRef]
20. **Manes C.** Nucleic acid synthesis in preimplantation rabbit embryos. III. A “dark period” immediately following fertilization, and the early predominance low molecular weight RNA synthesis. *J Exp Zool* 1977; **201**: 247–257. [Medline] [CrossRef]
21. **Baran V, Mercier Y, Renard JP, Fléchon JE.** Nucleolar substructures of rabbit cleaving embryos: an immunocytochemical study. *Mol Reprod Dev* 1997; **48**: 34–44. [Medline] [CrossRef]
22. **Collings DA, Carter CN, Rink JC, Scott AC, Wyatt SE, Allen NS.** Plant nuclei can contain extensive grooves and invaginations. *Plant Cell* 2000; **12**: 2425–2440. [Medline] [CrossRef]
23. **Hernandez-Verdun D.** The nucleolus: a model for the organization of nuclear functions. *Histochem Cell Biol* 2006; **126**: 135–148. [Medline] [CrossRef]
24. **Ndiaye M, Mattei X.** Process of nuclear envelope reduction in spermiogenesis of a mosquito, Culex tigripes. *Mol Reprod Dev* 1993; **34**: 416–419. [Medline] [CrossRef]
25. **Bodoor K, Shaikh S, Salina D, Raharjo WH, Bastos R, Lohka M, Burke B.** Sequential recruitment of NPC proteins to the nuclear periphery at the end of mitosis. *J Cell Sci* 1999; **112**: 2253–2264. [Medline]